JOURNAL OF CATALYSIS **167,** 57–65 (1997)
ARTICLE NO. CA971545

Working Mechanism of Oxide Catalysts in the Partial Oxidation of Methane to Formaldehyde

I. Catalytic Behaviour of SiO_2, MoO_3/SiO_2, V_2O_5/SiO_2, TiO_2, and V_2O_5/TiO_2 Systems

Adolfo Parmaliana*,† and Francesco Arena*

*Dipartimento di Chimica Industriale, Università degli Studi di Messina, Salita Sperone c.p. 29, 1-98166 S. Agata, Messina, Italy; and †Istituto CNR-TAE, Salita S. Lucia 39, 1-98126 S. Lucia, Messina, Italy

Received February 27, 1996; revised November 12, 1996; accepted December 2, 1996

The catalytic behaviour of SiO_2, MoO_3/SiO_2, V_2O_5/SiO_2, TiO_2, and V_2O_5/TiO_2 systems in the partial oxidation of methane to formaldehyde with O_2 (MPO) has been systematically evaluated by temperature programmed reaction (TPR) measurements in the range 400–800°C. The effects of MoO_3 (2–7 wt%) and V_2O_5 (2–20 wt%) loading on the surface reactivity of the SiO_2 support have been assessed. A sequential reaction path ($CH_4 \rightarrow HCHO \rightarrow CO \rightarrow CO_2$) accounts for the formation of oxygenated products on all SiO_2 based oxide catalysts at $T < 650$°C, while a surface assisted gas-phase reaction pathway leads to the formation of minor amounts of C_2 products both on SiO_2 and MoO_3/SiO_2 catalysts at $T \geq 700$°C. MoO_3 depresses the specific surface activity (SSA, $nmol_{CH_4}\ s^{-1}\ m^{-2}$) of the bare silica at $T < 650$°C, while V_2O_5 acts as a promoter of the SSA of both SiO_2 and TiO_2 carriers at any T. The maximum SSA on medium loaded (5–10 wt%) V_2O_5/SiO_2 catalysts has been observed though HCHO selectivity steadily decreases with V_2O_5 loading. The marked redox behaviour of TiO_2 based catalysts enables the prevailing formation of CO_x at any T. The different reactivity of SiO_2 and TiO_2 supports as well as their influence on the catalytic performance of supported oxide systems have been discussed.

INTRODUCTION

The great interest focused during last decade on the catalytic partial oxidation of methane to formaldehyde with O_2 (MPO) has been mainly aimed at discovering very active and/or selective catalysts, while less attention has been devoted to defining the surface reaction mechanism. Although a great variety of unpromoted and promoted oxide catalysts has been claimed to be effective in the MPO (1), it is generally recognized that silica based catalysts exhibit the best performance in catalysing the formation of partial oxidation products (2–6). In fact, the use of alternative carriers such as Al_2O_3 (7) or TiO_2 (6), unless provided very active systems, in no case denoted a satisfactory performance towards HCHO formation (6, 7). Further, since the various commercial silica samples revealed marked differences in their reactivities (5, 6), the addition of MoO_3, V_2O_5, and other transition metal oxides on the own reactivity of silica supports results in a promoting or poisoning effect (8–14).

The catalytic properties of supported MoO_3 and V_2O_5 are strongly affected by the metal oxide–support interaction which controls both reducibility and dispersion of the active phase (10, 12–17). In particular, the higher activity and selectivity of supported catalysts with respect to bulk oxides in MPO (6, 7, 14), as well as in other partial oxidation reactions (15–18), arise from the formation of easily reducible mixed support–metal oxide phases (10–13, 15–17) ensuring an easier occurrence of redox cycles under reaction conditions. Then, although a general agreement has been reached on the factors controlling the reactivity of oxide catalysts in selective oxidation reactions (15–18), the higher temperatures at which the MPO is usually carried out (500–700°C) with respect to the partial oxidation of higher hydrocarbons ($T \leq 450$°C) do not allow prediction of the catalytic behaviour of MPO catalysts in the light of previously established rules (18).

Therefore this paper is aimed at (i) providing basic insights into the influences of the support (i.e., SiO_2 and TiO_2) and oxide loading on the reactivity of MoO_3 and V_2O_5 based systems in the MPO, (ii) relating thoroughly the catalytic pattern of the studied systems with the redox and surface properties, and (iii) shedding light into the "working mechanism" of oxide catalysts in the MPO.

EXPERIMENTAL

Catalysts

MoO_3/SiO_2 (MPS), V_2O_5/SiO_2 (VPS), and V_2O_5/TiO_2 (VT) catalysts were prepared by incipient wetness impregnation of "precipitated" silica, PS, (Si 4-5P Grade, Akzo product; BET surface area, 400 $m^2\ g^{-1}$) and TiO_2 (GVA-500, Corning Glass product, BET surface area, 45 $m^2\ g^{-1}$)

0021-9517/97 $25.00

TABLE 1

List of Studied Catalysts

Catalyst	Chemical composition (wt%)	BET SA ($m^2\ g^{-1}$)
PS	SiO_2	400
MPS 2	2.0% MoO_3/SiO_2	300
MPS 4	4.0% MoO_3/SiO_2	190
MPS 7	7.0% MoO_3/SiO_2	75
VPS 2	2.1% V_2O_5/SiO_2	260
VPS 5	5.3% V_2O_5/SiO_2	230
VPS 10	10.8% V_2O_5/SiO_2	198
VPS 20	20.8% V_2O_5/SiO_2	193
TiO_2	TiO_2	45
VT 2	2.0% V_2O_5/TiO_2	48

samples with basic aqueous solution (pH ≈ 11) of ammonium heptamolybdate or ammonium metavanadate, respectively. After impregnation all the catalysts were dried at 110°C for 24 h and then air calcined at 600°C for 16 h. All the catalysts were pressed at 400 bar and subsequently crushed and sieved to the used particle size fraction (16–25 mesh). MoO_3 and V_2O_5 loadings were determined by atomic absorption spectroscopy (AAS). The list of samples investigated along with the relative oxide loading and BET surface area values are presented in Table 1.

Catalytic Measurements

Temperature programmed reaction (TPR) measurements (19, 20) were performed in a conventional flow apparatus using a linear quartz microreactor connected on line with a Thermolab (Fisons Instruments) quadrupole mass spectrometer (QMS) for continuous scanning of the reaction stream (transit time < 0.5 s). TPR tests were run in the T range 400–800°C by using 0.05 g of catalyst, a heating rate (β) of 10°C min^{-1}, and a reaction mixture $He/CH_4/O_2$ in the molar ratio 7:2:1 flowing at a rate of 50 or 100 STP $cm^3\ min^{-1}$, which corresponds to a contact time, τ, equal to 0.166 or 0.083 s, respectively. Before TPR tests, catalyst samples were conditioned *in situ* at 600°C for 1 h in a 15% O_2/He flow.

Mass spectra were recorded in multiple ion monitoring (MIM) mode using the SEM amplifier operating at 1500 V and an ionization potential of −70 V (total pressure, 8×10^{-9} bar). TPR spectra were obtained by acquiring the signals relative to the following mass-to-charge ratio (m/z) values: 2 (H_2), 4 (He), 15 (CH_3), 17 (OH), 25 (C_2H), 28 (CO), 29 (CHO), 30 (HCHO), 32 (O_2), and 44 (CO_2). The CH_4 consumption was revealed by the CH_3 (m/z, 15) signal, while HCHO and C_2 products (C_2H_6 and C_2H_4) have been detected by following the HCHO (m/z, 30) and C_2H (m/z, 25) masses, respectively. By using He as internal standard, CH_4 and O_2 conversion values at any temperature, T, were derived from the P_{CH_3}/P_{He} and P_{O_2}/P_{He} signal ratios, respectively,

$$CH_4\ \text{conv.} = 1 - \left[\frac{\left(P_{CH_3}/P_{He}\right)_T}{\left(P^*_{CH_3}/P^*_{He}\right)}\right] \qquad [1]$$

$$O_2\ \text{conv.} = 1 - \left[\frac{\left(P_{O_2}/P_{He}\right)_T}{\left(P^*_{O_2}/P^*_{He}\right)}\right], \qquad [1']$$

where P_i and P_i^* are the values of the instrumental signal of the species i at the temperature T and 400°C, respectively. The methane conversion value of ca. 24% ($CH_4/O_2 \approx 6$) was conventionally taken as the upper limit for kinetic analysis in order to rule out the constraints imposed by high conversions of the gas-phase oxygen.

For the calculation of the carbon mass-balance, the response factor ($A = [I \cdot R]^{-1}$) for CH_3, HCHO, C_2H, CO, and CO_2 species was determined from the relative sensitivity factor (R) of such species with respect to N_2 and the cracking pattern (i.e., abundance of the fragment considered, m/z, in the mass spectrum, l) of CH_4, HCHO, C_2H_6, C_2H_4, CO, and CO_2 molecules, assuming a constant contribution of 70% of C_2H_6 (30% of C_2H_4) on the total C_2 formation. Then, the response factors 0.62, 3.44, 34.41, 1.0, and 1.19 for m/z 15 (CH_3), 30 (HCHO), 25 (C_2H), 28 (CO), and 44 (CO_2), respectively, were obtained. The intensities of the CO (m/z, 28) and HCHO (m/z, 30) signals were also corrected for the relative contribution of C_2 products. That is, response factors equal to 0.5 and 0.2 on the total C_2 formation were considered as contribution of C_2 products to 28 and 30 m/z values, respectively. The methane conversion values, derived from the carbon–mass balance according to

$$CH_4\ \text{conv.} = \frac{\sum_i \cdot n_i \cdot A_i \cdot P_i}{\left[\sum_i n_i \cdot A_i \cdot P_i + \left(A_{CH_3} \cdot P_{CH_3}\right)\right]} \qquad [2]$$

where n_i is the number of C atoms in the product molecule, resulted ever in a good agreement (±10%) with those calculated from the P_{CH_3}/P_{He} ratio. The reliability of the carbon–mass balance has allowed us to calculate the product selectivity (S_i) by the following expression:

$$S_i = \frac{n_i \cdot A_i \cdot P_i}{\sum_i n_i \cdot A_i \cdot P_i}. \qquad [3]$$

Finally, the onset temperature ($T_{o,i}$) of product formation, conventionally taken as the temperature at which the concentration of the product i in the stream resulted ca. 50 ppm, has been timely determined with an accuracy of ±5°C by performing a suitable background subtraction procedure in the TPR spectra.

TABLE 2

Methane Partial Oxidation on SiO_2 Based Oxide Catalysts: Onset Temperature of Product Formation

Catalyst	$T_{o,HCHO}$ (°C)	$T_{o,CO}$ (°C)	T_{o,CO_2} (°C)	T_{o,C_2} (°C)	T_{o,H_2} (°C)
Blank test[a]	600	650	—	710	710
PS	480	510	560	690	690
MPS 2	490	530	580	700	700
MPS 4	530	540	560	730	730
MPS 7	530	600	660	750	750
VPS 2	460	500	530	740	740
VPS 5	450	480	520	730	730
VPS 10	470	480	530	730	730
VPS 20	470	475	540	750	750

[a] Data taken from Ref. (20).

RESULTS

Onset Temperature ($T_{o,i}$) of Product Formation on SiO_2 and TiO_2 Supported Catalysts

The onset temperatures at which the bare silica and differently loaded MoO_3/SiO_2 and V_2O_5/SiO_2 catalysts promote the formation of HCHO ($T_{o,HCHO}$), CO($T_{o,CO}$), CO_2 (T_{o,CO_2}), C_2 (T_{o,C_2}), and H_2(T_{o,H_2}) are listed in Table 2. For the sake of comparison also the onset temperatures of product formation in the blank test are shown therein (20). It is evident that addition of V_2O_5 (2–20 wt%) to the PS support promotes the formation of HCHO at T lower than that found for the bare PS sample (480°C). Namely, for V_2O_5 loading up to 5 wt% (VPS 5), $T_{o,HCHO}$ decreases from 480°C (PS) to 460 (VPS 2) and 450°C (VPS 5); thereafter it slightly rises, keeping unchanged on VPS 10 (470°C) and VPS 20 (470°C) samples. For MPS catalysts an opposite shift of $T_{o,HCHO}$ to higher T is found (Table 2). At T immediately higher than $T_{o,HCHO}$ all the systems catalyse the formation of CO ($T_{o,CO}$), while CO_2 is detected at T further higher than those found for the formation of both HCHO and CO. Then, the formation of C_2 products (T_{o,C_2}), paralleled by a concomitant rise in the H_2 signal, has been recorded at 690, 700, 730 and 750°C for PS, MPS 2, MPS 4, and MPS 7 catalysts, respectively.

The onset temperatures of product formation of TiO_2 based catalysts are listed in Table 3. The formation of CO on TiO_2 and VT 2 samples occurs at 430 and 405°C, respectively, while formaldehyde ($T_{o,HCHO} = 500$°C) and carbon dioxide ($T_{o,CO_2} = 510$°C) are detected at considerably higher T. Only trace amounts of C_2 products ((T_{o,C_2})) are observed on TiO_2 system at $T \geq 660$°C.

TABLE 3

Methane Partial Oxidation on TiO_2 Based Oxide Catalysts: Onset Temperature of Product Formation

Catalyst	$T_{o,CO}$ (°C)	$T_{o,HCHO}$ (°C)	T_{o,CO_2} (°C)	T_{o,C_2} (°C)	T_{o,H_2} (°C)
TiO_2	430	500	510	660	650
VT 2	405	500	510	—	—

TABLE 4

Apparent Activation Energy Values of MPO on PS, TiO_2, VT 2, and VPS 2 Catalysts

Catalyst	T range (°C)	No. of exp. points[a]	E_{app} (kcal mol^{-1})
PS	550–800	26	34 ± 2
TiO_2	550–800	26	28 ± 2
VPS 2	550–720	18	39 ± 4
VT 2	550–720	18	34 ± 2

[a] Equally spaced (10°C) over the whole T range.

Activity of SiO_2 and TiO_2 Supported V_2O_5 Catalysts

The specific surface activity (SSA, nmol$_{CH_4}$ s^{-1} m^{-2}) and product selectivity as a function of reaction temperature (T) for PS (a), VPS 2 (b), TiO_2 (c), and VT 2 (d) catalysts are shown in Fig. 1. The values of the apparent activation energy (E_{app}) obtained from the related Arrhenius plots are reported in Table 4, while the values of CH_4 conversion and product selectivity of the bare TiO_2 sample in the range 600–800°C at contact time (τ) of 0.083 and 0.166 s are outlined in Table 5. These results evidentiate that:

(i) The bare PS support exhibits a considerable SSA regularly increasing with T up to a value of 90 nmol$_{CH_4}$ s^{-1} m^{-2} at 800°C (CH_4 conv. $\approx$ 24%; O_2 conv. $\approx$ 70%). The HCHO selectivity decreases monotonically with T from 100% ($T \leq 500$°C) to a value of 10% ca. at 800°C, while the selectivities to CO and CO_2 rise with T reaching the values of 80 and 10% ca., respectively. The value of E_{app} in the range 550–800°C is 34 kcal mol^{-1}.

(ii) Addition of 2 wt% of V_2O_5 to PS carrier (Fig. 1b) markedly enhances the surface activity of the support at any T: at 710°C the SSA of the VPS 2 system attains the

TABLE 5

Influence of the Contact Time (τ) on CH_4 Conversion and Product Selectivity in the MPO on TiO_2 Sample at Various T

τ (s)	T (°C)	CH_4 conversion (%)	Selectivity (%)		
			HCHO	CO	CO_2
0.083	600	0.4	12	87	1
	700	3.1	13	81	6
	800	9.1	9	76	15
0.166	600	0.9	5	92	3
	700	7.0	5	86	9
	800	18.0	3	76	19

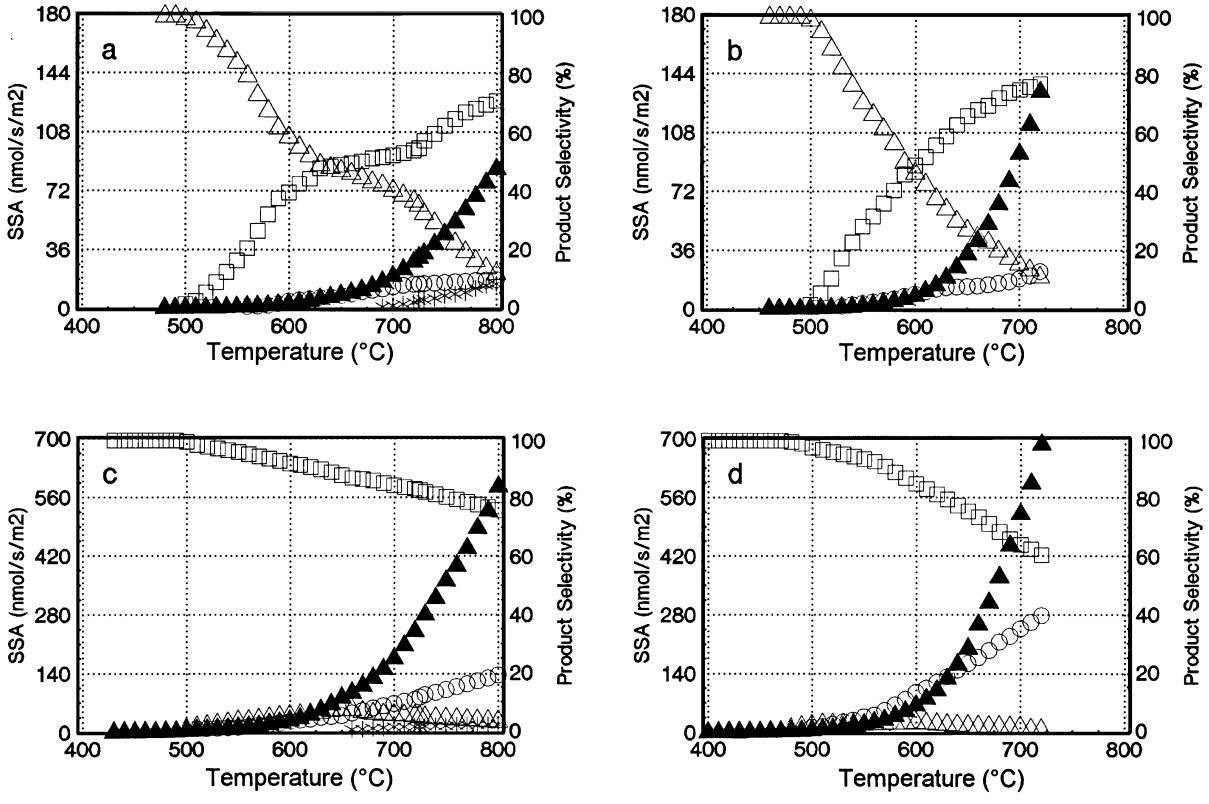

FIG. 1. Partial oxidation of methane to formaldehyde on (a) PS, (b) VPS 2, (c) TiO_2, and (d) VT 2 catalysts. (▲) Specific surface activity (SSA) and product selectivity (△, HCHO; □, CO; O, CO_2; ∗, C_2) vs T. Experimental conditions: β, 10°C min^{-1}; W_{cat}, 0.050 g; reaction mixture flow, 50 STP ml min^{-1} ($He : CH_4 : O_2 = 7 : 2 : 1$); τ, 0.166 s.

value of 135 $nmol_{CH_4}$ s^{-1} m^{-2} (CH_4 conv. ≈ 24%). Besides, a sharper decrease in the HCHO selectivity and a complementary growth of the CO selectivity with T are observed. No significant changes in the CO_2 selectivity values with respect to the bare PS are noticed ($S_{CO_2} \approx$ 10% at 710°C). The value of E_{app} in the range 550–720°C is equal to 39 kcal mol^{-1}, being then slightly higher than that found for the bare PS.

(iii) TiO_2 carrier ensures SSA values almost one order of magnitude higher than those of the unloaded PS sample at any T (cf. Figs. 1a and 1c). At 800°C the SSA attains a value of 580 $nmol_{CH_4}$ s^{-1} m^{-2} (CH_4 conv. ≈ 18%). CO is the main reaction product at any investigated T. The CO_2 selectivity rises regularly with T, reaching a maximum value of 20% at 800°C, while trace amounts of HCHO ($S_{HCHO} \approx$ 7% at 650°C) are detected in the range 500–800°C. A decrease in contact time from 0.166 to 0.083 s enhances the HCHO selectivity causing then a slight lowering in CO_x selectivity (Table 5). The E_{app} value in the range 550–800°C is 28 kcal mol^{-1}.

(iv) Addition of 2 wt% of V_2O_5 promotes the reactivity of TiO_2 carrier at any T (Fig. 1d) determining a rise in the E_{app} (34 kcal mol^{-1}). At 720°C the SSA value is equal to 680 $nmol_{CH_4}$ s^{-1} m^{-2} (CH_4 conv. ≈ 24%). CO is the main reaction product at any T. However, with respect to TiO_2 sample (Fig. 1c) a steeper decrease in CO selectivity with T, counterbalanced by a faster growth in CO_2 formation (Fig. 1d), is observed. Trace amounts of HCHO ($S_{HCHO} \approx$ 2% at 600°C) are detected in the range 500–700°C.

Influence of the Oxide Loading on the Catalytic Pattern of MoO_3/SiO_2 and V_2O_5/SiO_2 Catalysts

Catalytic activity. The catalytic activity of differently loaded MPS and VPS samples in the range 500–800°C, expressed in terms of normalised specific surface activity, NSSA ($NSSA = SSA_i/SSA_{PS}$, where SSA_i and SSA_{PS} are the specific surface activity of the catalyst i and bare PS support, respectively), is compared in Fig. 2. It is evident that any V_2O_5 loading promotes the surface reactivity of the PS at any T (log NSSA > 0) according to the following reactivity scale:

$$VPS\,5 > VPS\,10 > VPS\,2 \approx VPS\,20 > PS.$$

CH_4 conversion values close to 24% are attained at $T \approx$ 700°C on all VPS catalysts.

By contrast, MoO_3 exerts a negative effect on the SSA of the PS catalyst (log NSSA < 0) at $T <$ 650°C, while it

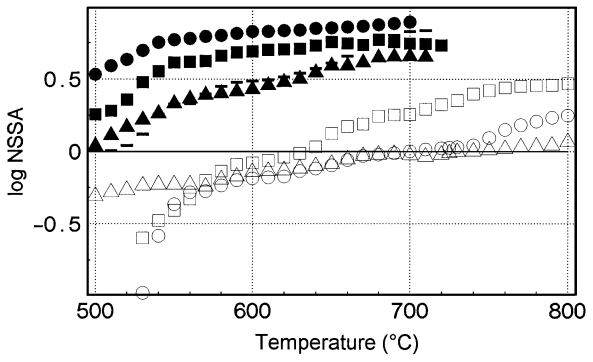

FIG. 2. Partial oxidation of methane to formaldehyde on (—) PS, (△) MPS 2, (○) MPS 4, (□) MPS 7, (▲) VPS 2, (●) VPS 5, (■) VPS 10, and (▬) VPS 20 catalysts. Logarithm of the normalised specific surface activity (NSSA) vs T.

promotes the SSA of the PS sample (log NSSA > 0) at $T > 700$°C. Namely, the increasing trend of the NSSA with T results more enhanced for the MPS 7 sample (Fig. 2).

The apparent activation energy (E_{app}) on the MPS and VPS catalysts are differently affected by the oxide loading, as shown in Table 6. In particular, for the MPS catalysts the E_{app} rises monotonically with the MoO_3 loading, going from 38 (MPS 2) to 47 kcal mol^{-1} (MPS 7). The V_2O_5 loading exerts a peculiar influence on the E_{app} of the VPS catalysts. In fact, the addition of 2–10 wt% of V_2O_5 to PS carrier results in a slight increase of E_{app} value (35–39 kcal mol^{-1}), while the highest value E_{app} (47 kcal mol^{-1}) is found for the VPS 20 sample.

Selectivity pattern. The HCHO selectivity as a function of both SSA and CH_4 conversion for MPS and VPS catalysts is shown in Figs. 3a and 3b, respectively. The trend of HCHO selectivity with SSA of MPS and VPS catalysts is not significantly different from that of the bare PS for MoO_3 and V_2O_5 loadings up to 4 and 10 wt%, respectively. Medium loaded MPS 7 and highly loaded VPS 20 samples result in the most and the least selective systems respectively (Fig. 3a). For MPS 2 and MPS 4 catalysts, the relationship between HCHO selectivity and CH_4 conversion (Fig. 3b) is similar to that of the unloaded PS, whereas for the MPS 7 sample a significant improvement in HCHO selectivity at conversion levels lower than 3% is observed. By contrast, at the same level of CH_4 conversion, a progressive decline in HCHO selectivity with V_2O_5 loading occurs on VPS catalysts (Fig. 3b).

TABLE 6

Apparent Activation Energy Values of MPO on MoO_3/SiO_2 (MPS) and V_2O_5/SiO_2 (VPS) Catalysts

Catalyst	T range (°C)	No. of exp. points[a]	E_{app} (kcal mol^{-1})
Blank test[b]	690–800	12	52 ± 4
PS	550–800	26	34 ± 2
MPS 2	550–800	26	38 ± 3
MPS 4	550–800	26	43 ± 1
MPS 7	550–800	26	47 ± 4
VPS 2	550–720	18	39 ± 4
VPS 5	550–700	16	35 ± 3
VPS 10	550–720	18	36 ± 4
VPS 20	550–710	17	47 ± 2

[a] Equally spaced (10°C) over the whole T range.
[b] E_{app} value calculated from data taken from Ref. (20).

TABLE 7

Methane Partial Oxidation on MPS and VPS Catalysts: Relative Rate of CO and CO_2 Formation in the Range 600–800°C

Catalyst	r_{CO}/r	r_{CO_2}/r	r_{CO_2}/r_{CO}	$[(r_{CO} + r_{CO_2})/r]$
PS	0.69	0.10	0.14	0.79
MPS 2	0.67	0.12	0.18	0.79
MPS 4	0.57	0.18	0.31	0.75
MPS 7	0.63	0.12	0.19	0.75
VPS 2	0.79	0.11	0.14	0.90
VPS 5	0.83	0.15	0.18	0.98
VPS 10	0.84	0.16	0.19	1.00
VPS 20	0.51	0.49	0.95	1.00

Note. $\tau = 0.166$ s; r_{CO}, rate of CO formation, 10^{-6} $mol_{CO}/s/g_{cat}$; r_{CO_2}, rate of CO_2 formation, 10^{-6} $mol_{CO_2}/s/g_{cat}$; r, reaction rate, 10^{-6} $mol_{CH_4}/s/g_{cat}$.

The CO_x selectivity pattern of MPS and VPS catalysts in the range 600–800°C has been probed by plotting the rate of formation of both CO (r_{CO}) and CO_2 (r_{CO_2}) as a function of the reaction rate (r): r_{CO} and r_{CO_2} rise with r according to a straight-line relationship for all the studied systems. The values of the slope of r_{CO}/r, r_{CO_2}/r, r_{CO_2}/r_{CO}, and $[(r_{CO} + r_{CO_2})/r]$ relationships are listed in Table 7. In spite of the qualitative character of such analysis, the above data can be taken as an index of the functionality of the various systems in driving the formation of CO_x. Taking into account the bare PS as reference system, it is evident that an increase in the V_2O_5 loading from 0 (PS) to 10% (VPS 10) yields a slight increase in both the relative rate of CO ($r_{CO}/r > 0.69$) and CO_2 ($r_{CO_2}/r > 0.10$) formation. Also the r_{CO_2}/r_{CO} value increases slightly up to a loading of 10 wt% (from 0.14 on PS to 0.19 on VPS 10 sample); thereafter, on VPS 20 sample it attains the value of 0.95 because of a steep lowering in rate of CO formation ($r_{CO}/r = 0.51$) and a concomitant marked growth in the rate of CO_2 formation ($r_{CO_2}/r = 0.49$). On the MPS catalysts a slight rise in the r_{CO_2}/r and a lowering in the r_{CO}/r values with reference to the bare PS are observed. The extent of this effect is more pronounced for the MPS 4 sample (Table 7), as indicated by its r_{CO_2}/r_{CO} value (0.31). Besides, it is evident that the overall rate of CO_x formation $[(r_{CO} + r_{CO_2})/r]$ of PS (0.79) is practically not affected by the MoO_3 addition (0.75–0.79), while it is markedly enhanced by V_2O_5 (0.90–1.00).

TPR measurements provide evidences of a different behaviour of the oxide catalysts towards the formation of C_2

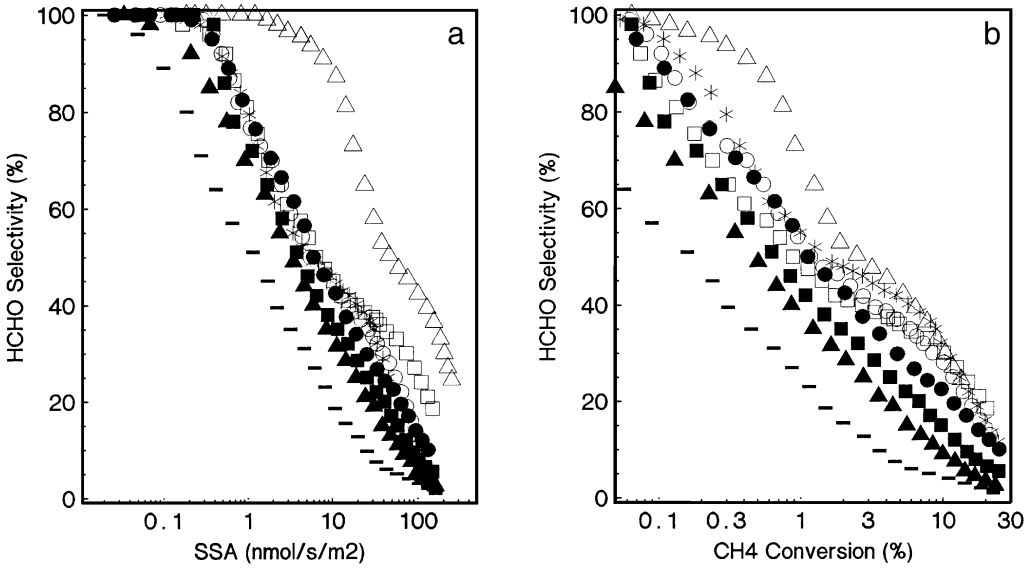

FIG. 3. Partial oxidation of methane to formaldehyde on PS (∗), MPS 2 (○), MPS 4 (□), MPS 7 (△), VPS 2 (●), VPS 5 (■), VPS 10 (▲), and VPS 20 (▬) catalysts in the range 400–800°C. HCHO selectivity vs SSA (a) and CH_4 conversion (b).

products. In fact, both PS sample (Fig. 2a) and MPS systems catalyse the formation of C_2 products at $T \geq 700$°C. The C_2 selectivity reaches a value of ca. 10% at 800°C on the PS sample and it lowers upon the MoO_3 loading increases. On VPS catalysts no C_2 formation is detected up to 730°C, while at higher T a slight C_2 formation, in concomitance with the full gas-phase O_2 consumption, is noticed (20).

HCHO yield. The performance of the studied catalysts in MPO is compared in Table 8 in terms of HCHO surface productivity (SP_{HCHO}, nmol m^{-2} s^{-1}) and space time yield (STY_{HCHO}, g kg_{cat}^{-1} h^{-1}) at different T. For the sake of completeness also the values of methane conversion and HCHO selectivity are reported.

For V_2O_5 loadings <10% an improvement in both SP_{HCHO} and STY_{HCHO} with respect to PS is observed at $T \leq 650$°C. At higher loading levels, the STY_{HCHO} of VPS catalysts steeply decreases, becoming even lower than that of PS. At $T > 700$°C, the MPS catalysts ensure STY_{HCHO}'s (450–570) and SP_{HCHO}'s higher than those of the bare PS sample; however, SP_{HCHO} values considerably higher than those of the PS support are already attained on MPS 7 catalyst at $T \geq 600$°C.

DISCUSSION

Reaction Path of the MPO on SiO_2 Based Oxide Catalysts

The activity scale of silica supported MoO_3 and V_2O_5 catalysts, based on the inverse sequence of $T_{o,HCHO}$ values (Table 2),

$$\text{VPS 5} > \text{VPS 2} < \text{VPS 20} \cong \text{VPS 10} > \text{PS} > \text{MPS 2} > \text{MPS 4} \cong \text{MPS 7},$$

fully accounts for the opposite effect exerted by MoO_3 and V_2O_5 promoters on the own activity of the bare PS sample (6, 11, 12, 19, 20). Such data indicate that the negative effect of MoO_3 rises with the level of loading, while the promoting effect of V_2O_5 reaches its maximum on the medium loaded VPS 5 catalyst. Even if the addition of MoO_3 and V_2O_5 promoters differently affects the own activity of the PS carrier, the same sequence of the onset temperature of product formation,

$$T_{o,HCHO} < T_{o,CO} < T_{o,CO_2},$$

proves that HCHO is the primary product of the MPO on both MPS and VPS catalysts (8, 9, 14, 20–22). The subsequent formation of CO ($T_{o,CO}$) at T slightly higher than $T_{o,HCHO}$ suggests that such product arises from the consecutive oxidation of HCHO mainly on the catalyst surface (1, 8, 9, 14, 20–22). whereas the formation of carbon dioxide at $T > T_{o,CO}$ signals that the total oxidation product mainly comes from the consecutive oxidation of carbon monoxide according to the following sequential reaction path (1, 9, 20):

$$CH_4 \rightarrow HCHO \rightarrow CO \rightarrow CO_2.$$

Previous kinetic studies of the MPO provided evidences of the occurrence of a consecutive and a parallel reaction path accounting for the formation of carbon dioxide on V_2O_5/SiO_2 (9, 21) and MoO_3/SiO_2 (8, 14, 22) catalysts, respectively. However, it should be considered that the unreactive "pyrolitic" silica, generally used as support in MoO_3/SiO_2 catalysts (8, 14, 22), does not contribute to the overall reaction network, whereas the reactivity of MPS catalysts at $T \leq 650$°C (Fig. 2) must be ascribed to

TABLE 8

Methane Conversion, HCHO Selectivity, Surface Productivity (SP_{HCHO}), and Space Time Yield (STY_{HCHO}) to HCHO in MPO on MoO_3 and V_2O_5 Supported PS Catalysts at Various T

Catalyst	T (°C)	CH_4 conv. (%)	HCHO sel. (%)	SP_{HCHO} (nmol m^{-2} s^{-1})	STY_{HCHO} (g kg_{cat}^{-1} h^{-1})
PS	600	0.78	58.5	1.6	73
	650	2.34	47.0	3.8	164
	700	5.70	40.2	7.9	343
	800	24.6	11.5	9.8	420
MPS 2	600	0.42	69.8	1.4	44
	650	1.45	47.8	3.2	104
	700	4.00	39.5	7.4	239
	800	21.5	13.0	13.9	450
MPS 4	600	0.24	70.0	1.1	23
	650	0.89	50.0	3.2	67
	700	2.72	40.0	7.6	144
	800	20.5	18.0	27.7	568
MPS 7	600	0.12	99.0	2.2	18
	650	0.58	91.0	9.9	27
	700	1.90	58.0	20.6	96
	800	13.5	24.5	61.9	500
VPS 2	600	1.49	46.3	3.2	92
	650	6.30	26.7	9.1	255
	700	17.8	15.0	14.2	404
VPS 5	600	3.30	28.5	5.7	128
	650	10.0	15.0	9.0	227
	700	24.7	5.5	8.2	195
VPS 10	600	2.10	28.5	4.2	98
	650	7.00	13.0	6.4	136
	700	16.8	4.5	5.3	113
VPS 20	600	1.15	23.0	4.0	40
	650	4.60	7.5	2.5	52
	700	18.5	2.0	2.7	55

Note. $\tau = 0.166$ s.

the functionality of the uncovered PS surface (4, 6, 11, 12, 19, 20) which implies the above sequential reaction path (20).

The activity–selectivity pattern of the studied catalysts proves the *structure sensitivity* character of the MPO over oxide systems. In fact, even if both specific surface activity (Fig. 2) and CH_4 conversion (Table 8) attain the highest level on the medium loaded V_2O_5/SiO_2 system (VPS 5), by increasing V_2O_5 loading a rise in the selectivity to CO_x (Table 7) along with a complementary decrease in HCHO selectivity (Fig. 3) have been pointed out. These results match with previous literature data showing the existence of an optimum loading (1–8 wt%) which ensures the best activity and selectivity of V_2O_5/SiO_2 catalysts in MPO (10, 13). Namely, the occurrence of a more effective reduction–oxidation cycle from V^{5+} to V^{4+}/V^{3+}, associated with the presence of tetrahedral vanadate species on the silica surface, has been invoked to explain the highest performance of the medium loaded V_2O_5/SiO_2 catalysts in the title reaction (10). On this account, the highest value of E_{app} (47 kcal mol^{-1}) for VPS 20 sample reflects a lower effectiveness of the highly loaded system in CH_4 activation at $T \leq 650$°C (Fig. 2), while low-medium loaded (2–10 wt%) VPS catalysts enable the easier occurrence of the aforesaid redox cycle, resulting in lower E_{app} values (35–39 kcal mol^{-1}).

On the whole, the above findings allow us to infer that the activity–selectivity pattern of differently loaded VPS catalysts is attributable to different "surface V structures" (15, 16), each of them features a peculiar catalytic action in MPO. Indeed, the negative influence of the oxide loading on the HCHO selectivity (13) should be mostly a consequence of the lower oxide dispersion which implies the stabilization of surface structures promoting the formation of total oxidation products (10, 13, 16, 21). Then, the regular increase in the rate of formation of both CO and CO_2 for low–medium loaded (2–10 wt%) VPS catalysts (Table 7) is a consequence of the enhanced activity, while the high CO_2 selectivity of VPS 20 sample (Table 7) reflects an extensive formation of V_2O_5 crystallites (16) which depress the formation of partial oxidation products without any beneficial influence on the activity.

MoO_3 reduces the SSA of the bare PS at $T < 650$°C acting as a promoter at higher T (Fig. 2). This effect depends upon the loading level (Fig. 2) as confirmed by the progressive rise in the E_{app} value of MPS catalysts with MoO_3 loading (Table 6). Therefore, these findings indicate a substantial inability of the MoO_3 promoter in undergoing the redox cycle under reaction conditions at $T \leq 650$°C. Moreover, the trend of HCHO selectivity vs both SSA and CH_4 conversion for MPS 2 and MPS 4 samples is similar to that of the bare PS (Fig. 3), while the highest HCHO selectivity of MPS 7 catalyst can be related with the catalytic functionality of "Mo=O" sites of MoO_3 crystallites which are less active and more selective than "Mo–O–Mo" bridging sites of "dispersed Mo species" (14). On the other hand, it has been ascertained that higher temperatures exert a beneficial influence on the HCHO selectivity at a given value of CH_4 conversion (8, 9), likely because of an easier desorption of the HCHO intermediate; then the highest selectivity of the MPS 7 sample could be a consequence of its lowest activity level. Furthermore, the low BET surface area value of MPS 7 sample (Table 1) rules out any significant contribution of the silica surface in the reaction network (see *infra*). The data reported in Table 7 also indicate that the MoO_3 addition does not affect the overall selectivity to CO_x $[(r_{CO} + r_{CO_2})/r]$ of the bare PS, though MPS catalysts exhibit a higher tendency towards CO_2 formation. Such enhancement in the rate of CO_2 formation (Table 7), more evident for MPS 4 catalyst, is diagnostic of the peculiarity of MPS systems in driving total oxidation of CH_4 and/or CO to CO_2 (8, 14).

Although the SSA values of MPS catalysts at 650°C (6.5–10.9 nmol m^{-2} s^{-1}) are analogous to those obtained by Smith *et al.* on similar systems (14), a direct comparison of our results with those reported by other research groups (8, 14, 22) should be viewed cautiously, taking into account the reactivity of PS carrier (SSA = 8.1 nmol m^{-2} s^{-1} at 650°C). Namely, the similar activity–selectivity pattern of PS and MPS catalysts at $T \leq 700$°C (see Fig. 3 and Tables 7 and 8) proves the prevailing contribution of the "free" silica surface in the reactivity of MPS catalysts, while at $T > 700$°C the catalytic action of "MoO_3 species" (14) implies significant changes in the catalytic pattern of MPS samples with respect to PS support. Then, the different reactivity of silica supports (4, 6, 20) is the reason for the differences in the activity of MPS 4 and 4.5 wt% MoO_3 supported on fumed silica (MFS 4) samples at $T < 650$°C in spite of their similar BET surface area values (20). Further, it must be considered that the preparation method of silica, besides to determine the reactivity in MPO (4, 6, 20), likely affects the "surface distribution" and reactivity of thereon supported MoO_3 and V_2O_5 promoters.

Then, the bulk of the above results indicates that V_2O_5 addition enhances the formaldehyde productivity (i.e., SP_{HCHO} and STY_{HCHO}) of the PS carrier at $T \leq 700$°C owing to the promoting effect on the activity, while MoO_3 promoter enables higher STY_{HCHO} and SP_{HCHO} values at $T > 750$°C as a consequence of its higher HCHO selectivity (Table 8).

The concomitant formation of H_2 and C_2 products on both PS and MPS catalysts at $T \geq 700$°C suggests that coupling products likely arise from the stabilisation of CH_3· radicals on the "exposed" surface of the silica carrier (5, 20). The absence of these C_2 products on VPS catalysts up to 700°C (20) can be ascribed to the high capability of V_2O_5 based systems in providing large amounts of surface-activated oxygen species which are very reactive towards CH_3· radicals, enabling their prompt oxidation (11, 20, 23).

Comparison of the Reactivity of Bare and V_2O_5 Promoted SiO_2 and TiO_2 Catalysts

The different sequence of onset temperature of product formation observed on TiO_2 and VT 2 with respect to that of PS and VPS 2 catalyst samples (Table 3) confirms that the interaction occurring between the catalyst surface and reactants is crucial in determining the catalytic pattern of oxide systems in MPO. In particular, the data reported in Table 3, besides to point out that the main product of the MPO on TiO_2-based catalysts is carbon monoxide, indicate that these systems enable CH_4 activation ($T_{o,CO}$) at T lower than those observed for silica-based ones (Table 2). Such an evidence of a higher reactivity of TiO_2 and VT 2 catalysts is well supported by their SSA resulting quite higher than that of PS-based catalysts (Fig. 1). However, due to the great differences in the BET surface area of PS- and TiO_2-supported catalysts (Table 1), the activity level (in terms of CH_4 conversion) of TiO_2 and VT 2 catalysts, in the range 500–800°C, results lower or at least comparable with that of PS and VPS 2 catalysts. Then, it arises that the large CO selectivity of titania-based catalysts (Figs. 1c and 1d) is not a consequence of the inverse conversion–selectivity relationship (8, 9), but rather it reflects a marked oxidation strength of these systems towards HCHO. In fact, taking into account the positive influence of lower contact times on the HCHO selectivity of the bare TiO_2 carrier (Table 5) it can be argued that also on this system the MPO proceeds through the primary formation of the HCHO intermediate. Such a catalytic pattern of TiO_2 sample in MPO matches with the results of Wachs *et al.* in the partial oxidation of *o*-xylene to phtalic anhydride on V_2O_5/TiO_2 catalysts (17) according to which it can be inferred that the exposed sites of titania support cause the complete combustion of partial oxidation products. Therefore, the higher SSA of VT 2 sample with respect to that of VPS 2 catalyst (cf. Figs. 1b and 1d) stems from the different reactivity of TiO_2 and SiO_2 supports (15). Indeed, the addition of 2 wt% of V_2O_5 to PS (VPS 2) or TiO_2 (VT 2) results in a comparable promoting effect of the SSA of the related support (Fig. 1). Therefore, it can be concluded that the lower apparent activation energy values of TiO_2 and VT 2 catalysts with respect to those of the counterpart PS and VPS 2 samples (Table 4) arise from their higher reactivity at $T < 650$°C.

Finally, the formation of C_2 products on TiO_2 at $T > 650$°C (Fig. 1c) signals the occurrence of a reaction mechanism involving the coupling of methyl radicals, analogous to that catalyzed by the silica surface (5), even if the low C_2 selectivity ($S_{C_2} < 2\%$ at 800°C) of this system is a further probatory evidence of its marked oxidation strength.

CONCLUSIONS

The catalytic pattern of SiO_2, TiO_2, MoO_3/SiO_2, V_2O_5/SiO_2, and V_2O_5/TiO_2 catalysts in MPO has been investigated by temperature programmed reaction measurements providing basic insights into the influences of the reaction temperature, nature of the support, and loading level of MoO_3 and V_2O_5 promoters on the surface pathways of the title reaction.

In particular, the main results of this work can be summarised as follows:

1. V_2O_5 is a promoter of the specific surface activity of both "precipitated SiO_2" (PS) and TiO_2 carriers at any T.

2. At $T < 650$°C MoO_3 depresses the surface reactivity of PS, resulting in a promoter at higher T. The extent of these effects rises with MoO_3 loading.

3. The activity–selectivity pattern of MPS and VPS catalysts in the MPO is controlled by the oxide loading.

4. Titania exhibits a surface reactivity in MPO much higher than that of the "precipitated" silica.

5. The MPO proceeds on both PS- and TiO_2-based catalysts through the primary formation of HCHO, even if the latter systems exhibit a very poor HCHO selectivity at any *T*.

ACKNOWLEDGMENTS

The financial support to this work by EEC (Contract JOU2-CT92-0040) and MURST (Rome, Italy) is gratefully acknowledged.

REFERENCES

1. Krylov, O. V., *Catal. Today* **18**, 209 (1993).
2. Kasztelan, S., and Moffat, J. B., *J. Chem. Soc. Chem. Commun.* 1663 (1987).
3. Kastanas, G. N., Tsigidinos, G. A., and Schwank, J., *Appl. Catal.* **44**, 33 (1988).
4. Parmaliana, A., Frusteri, F., Miceli, D., Mezzapica, A., and Scurrell, M. S., *Appl. Catal.* **78**, L7 (1991).
5. Sun, Q., Herman, R. G., and Klier, K., *Catal. Lett.* **16**, 251 (1992).
6. Parmaliana, A., Frusteri, F., Mezzapica, A., Miceli, D., Scurrell, M. S., and Giordano, N., *J. Catal.* **143**, 262 (1993).
7. Koranne, M. M., Goodwin, J. G., and Marcelin, G., *J. Catal.* **148**, 378 (1994).
8. Spencer, N. D., *J. Catal.* **109**, 187 (1988).
9. Spencer, N. D., and Pereira, C. J., *J. Catal.* **116**, 399 (1989).
10. Kennedy, M., Sexton, A., Kartheuser, B., Mac Giolla Coda, E., McMonagle, J. B., and Hodnett, B. K., *Catal. Today* **13**, 447 (1992).
11. Parmaliana, A., Sokolovskii, V., Miceli, D., Arena, F., and Giordano, N., *in* "Catalytic Selective Oxidation" (S. T. Oyama and J. W. Hightower, Eds.), ACS Symp. Series 523, p. 43. Washington DC. 1993.
12. Miceli, D., Arena, F., Parmaliana, A., Scurrell, M. S., and Sokolovskii, V., *Catal. Lett.* **18**, 283 (1993).
13. Kartheuser, B., and Hodnett, B. K., *J. Chem. Soc. Chem. Commun.* 1093 (1993).
14. Smith, M. R., Zhang, L., Driscoll, S. A., and Ozkan, U. S., *Catal. Lett.* **19**, 1 (1993).
15. Deo, G., and Wachs, I. E., *J. Catal.* **129**, 307 (1991).
16. Owens, L., and Kung, H. H., *J. Catal.* **144**, 202 (1993).
17. Wachs, I. E., Saleh, R. Y., Chan, S. S., and Chersich, C. C., *Appl. Catal.* **15**, 339 (1985).
18. Sokolovkii, V., *Catal. Rev.-Sci. Eng.* **32**(1 and 2), 1 (1990).
19. Arena, F., Frusteri, F., Parmaliana, A., and Giordano, N., *J. Catal.* **143**, 299 (1993).
20. Arena, F., Frusteri, F., Parmaliana, A., and Giordano, N., *Appl. Catal. A General* **125**, 39 (1995).
21. Kartheuser, B., Hodnett, B. K., Zantoff, H., and Baerns, M., *Catal. Lett.* **21**, 209 (1993).
22. Mauti, R., and Mims, C. A., *Catal. Lett.* **21**, 201 (1993).
23. Parmaliana, A., Sokolovskii, V., Miceli, D., Arena, F., and Giordano, N., *J. Catal.* **148**, 514 (1994).